Boiler Ash of Oil Palm Shell as Adsorbent for Lead Adsorption

N. Nurdiansyah, Chusnul Hidayat*, Dian Anggraini Suroto

Department of Food and Agricultural Product Technology, Faculty of Agricultural Technology, Universitas Gadjah Mada, Jl. Flora No. 1, Bulaksumur, Yogyakarta 55281, Indonesia
*Corresponding author: Chusnul Hidayat, Email: chusnulhi@ugm.ac.id

Submitted: April 21, 2024; Revised: September 6, 2024, September 17, 2024, October 2, 2024; Accepted: October 3, 2024; Published: May 28, 2025

ABSTRACT

Palm oil shells and fibers are widely used as fuel for factory boiler furnaces. However, boiler ash residue produced is often underutilized. This study aims to explore the use of boiler bottom ash (BBA) as an adsorbent for the adsorption of lead (Pb) and its subsequent application in palm oil mill effluent (POME) purification for water dilution in crude palm oil (CPO) processing. BBA was activated using 0.2, 0.4, 0.6, and 0.8 mol/L potassium hydroxide (KOH) solutions for 24 hours, and the carbonation was conducted at 400°C for 60 minutes. Factors, such as the concentration of KOH for BBA activation, pH levels, adsorption temperature, adsorption kinetics, and the application of the adsorbent in POME purification for water dilution in the CPO processing model, were evaluated. The results showed that the optimal KOH concentration was 0.4 mol/L, as determined by SEM, EDX, and lead adsorption analysis. The maximum adsorbent capacity of approximately 0.43 mg/g was obtained at 50°C and pH 4.6, with an adsorption rate constant of 5.97 per minute. The results also showed that the adsorption process followed the Langmuir model. In addition, the adsorption activation energy and the Arrhenius constant values were -28675.82 J/mol and 0.0001, respectively. The use of POME filtrate for water dilution had no effect on the free fatty acids, water content, impurities, or DOBI (Deterioration Bleachability of Index) in CPO. Lead value showed significant differences in all treatments without dilution. These results indicate that BBA activated with KOH can function as an adsorbent to reduce lead content. POME purified with BBA adsorbent has the potential to be used as diluent water in CPO processing to reduce raw water use and ultimately decrease POME production.

Keywords: Adsorption; Adsorption isotherm; Boiler bottom ash; CPO quality; Lead;

INTRODUCTION

The expansion in several sectors and crude palm oil (CPO) output indirectly cause an increase in waste generation, including palm oil mill effluent (POME), empty fruit bunches, fiber, and palm kernel shells (Suparma et al., 2014). Several studies have shown that palm kernel shells and fiber can be used as boiler furnace fuel (Suparma et al., 2014). The combustion of shells and fibers in boiler furnaces occurs at high temperatures, leading to the production of by-products, such as fly ash and boiler bottom ash (BBA) (Prianti et al., 2015). BBA often accumulates at the bottom because it is not sucked up by the suction machine due to the larger mass. This waste is then disposed of on land around the palm oil mill, which increases the risk of environmental and health problems (Asyri et al., 2015).

According to previous studies, POME is often used as liquid fertilizer, but some are discharged into the environment after treatment. POME has been reported to contain organic compounds and heavy metals (Cd, Zn, Cu, and Pb) (Nursanti, 2013), which can contaminate the environment. Heavy metals, such as lead (Pb), have non-biodegradable characteristics and are easily

DOI: http://doi.org/10.22146/agritech.93514
ISSN 0216-0455 (Print), ISSN 2527-3825 (Online)

accumulated due to their high solubility, leading to high environmental damage (Ray & Shipley, 2015; Mahmud et al., 2016).

To address this problem, there are different ways to remove heavy metals from wastewater, including membrane separation, adsorption, and electrophoresis. Adsorption is often used to reduc heavy metal levels in wastewater (Wijaya et al., 2020), but it depends on the pH of the solution. A study showed the best results at pH 4, where adsorption followed the Freundlich model (Chen & Shi, 2017), and at pH 5, where adsorption followed the Langmuir model (Oktasari, 2018). Some materials commonly used as adsorbents are zeolites (Elysabeth et al., 2015), fly ash, and coal bottom ash (Praipipat et al., 2023), but these materials have some issues, such as having contaminants and not being very crystalline (Elysabeth et al., 2015). Fly ash and coal bottom ash also contain a lot of heavy metals (Firman et al., 2020).

BBA, produced from burning shells and fibers in boiler furnaces, can be used as an adsorbent (Khanday et al., 2017). The adsorbent's ability to work depends on its surface properties, surface area, pore size, and functional groups (Myllymaki et al., 2018). To improve the ability, the adsorbent needs to be modified using different activation materials (Gautam et al., 2014). Potassium hydroxide (KOH) is commonly used to activate BBA because it has a high carbon content. Several studies have shown that uncarbonated lignocellulosic materials are better activated with zinc chloride ($ZnCl_2$) as their high oxygen content facilitates interaction with the activator (Permata et al., 2019). Therefore, this study aims to explore the use of BBA as an adsorbent for the adsorption of lead and its subsequent application in POME purification for water dilution in CPO processing. The use of purified POME is expected to reduce the use of raw water in CPO processing. The amount of purified POME facilitates the creation of a sustainable palm oil processing industry. The influence of KOH content on BBA activation for lead adsorption, the impact of pH and adsorption temperature on lead metal ions, and the kinetics of adsorption were also examined in this study.

METHODS

Materials

POME, BBA, and CPO were obtained from a palm oil processing facility (Sambas, Indonesia). NaOH 99%, HNO3 65%, potassium hydroxide, acetic acid, sulfuric acid 90%, hydrogen peroxide 30%, n-hexane 95%, ethanol, iso-octane, oxalic acid, phenolphthalein indicator 1%, and alizarin red S monosodium salt were obtained from Merck KGaA (Darmstadt, Germany).

Research Instruments

Furnace (Eyela, TMF-2200, Japan), Drying Oven (Sanyo, MOV-112, Japan), Centrifuge (DILB, DMO636, Cina), UV-VIS Spectrophotometer (Shimadzu, UV-1280, Japan), Waterbath (Memmert, Germany), SEM JEOL JSM-6510LA dan Auto Coater JEOL JEC-3000FC, Disc mill (FFC-45, Indonesia).

Activation of Boiler Bottom Ash

BBA was activated using the method by Khanday et al. (2017). It was crushed using a disc mil and went through a 20-mesh sieve. The sample was then soaked in potassium hydroxide (KOH) solution with different amounts like 0.2, 0.4, 0.6, and 0.8 mol/L for 24 hours at room temperature, using a 1:1 weight ratio. Subsequently, BBA was filtered and washed with distilled water. Slowly, 1 mol/L acetic acid was added until the pH was 7, then drained. The drying process was carried out in an oven at 105°C for 60 minutes, followed by carbonation in a furnace at 400 °C for 60 minutes.

Solids Separation in Palm Oil Mill Effluent

POME was put in a 50 mL centrifuge tube and spun for 15 minutes at 3500 rpm, then the liquid was separated from the solids.

Effect of KOH for Boiler Botton Ash Activation on Adsorption of Lead Metal Ions

The activation of BBA was conducted following Khanday et al. (2017), with several changes, and the filtrate was diluted with distilled water at a 1:2 ratio. A total of 0.1 mol/L NaOH and 0.1 mol/L acetic acid solution was added to the filtrate until pH reached 4, 6, 7, and 8. Approximately 50 mL of each filtrate with pH levels of 4, 6, 7, and 8 was transferred into 5 Erlenmeyer flasks. Each Erlenmeyer flask received 1% activated BBA adsorbent at concentrations of 0, 0.2, 0.4, 0.6, and 0.8 mol/L. The combination of filtrate and adsorbent was incubated in a water bath at 60°C for 180 minutes with 120 shakes per minute. After adsorption, the filtrate was subjected to filtration with Whatman 1 µm porous paper. The filtrate was subsequently centrifuged at 3500 rpm for 15 minutes and was examined for lead metal ions with UV-Vis spectrophotometric method.

Effect of pH on Lead Adsorption

The activation of BBA followed a procedure similar to that of Khanday et al. (2017), with some modifications. Distilled water was mixed with the filtrate in a 1:2 ratio, followed by the addition of 0.1 mol/L NaOH and acetic acid to adjust the pH to 4.6, 7, and 8. Subsequently, 50

mL of each filtrate, corresponding to the different pH levels, was transferred into 5 Erlenmeyer flasks. In each flask, 1% BBA adsorbent, activated using KOH, was added in varying concentrations of 0, 0.2, 0.4, 0.6, and 0.8 mol/L. The filtrate and adsorbent mixture were then placed in a water bath at 60°C for 3 hours, with shaking at 120 rpm. The mixture was filtered using Whatman 1 µm porous paper and centrifuged at 3500 rpm for 15 minutes. Finally, the filtrate was analyzed for lead ions using UV-Vis spectrophotometry.

Effect of Adsorbent Mass on Lead Adsorption

The activation of BBA was carried out using the same procedures developed by Khanday et al. (2017), with some modifications. The filtrate was mixed with distilled water in a 1:2 ratio, followed by the gradual addition of 0.1 mol/L acetic acid until the pH reached 4.6. A 50 mL aliquot of the filtrate was then transferred into five 250 mL Erlenmeyer flasks. Different amounts of BBA adsorbent were added to each flask: 2%, 4%, 6%, 8%, and 10%. The filtrate containing lead ions was shaken in a water bath at 60°C for 3 hours, with a shaking speed of 120 rpm. Following this, the mixture was filtered through Whatman 1 µm porous paper and centrifuged at 3500 rpm for 15 minutes. The filtrate was then analyzed for lead ions using UV-Vis spectrophotometry .

Effect of Temperature on Adsorption of Lead Metal Ions

The activation of BBA followed a procedure similar to that of Khanday et al. (2017), with some modifications. A 50 mL lead solution at concentrations of 1, 3, 5, 7, 9, 12, and 15 ppm was prepared and placed into 250 mL Erlenmeyer flasks. To adjust the pH to 4.6, 0.1 mol/L acetic acid was added gradually. A total of 2% activated BBA adsorbent was introduced to the lead solution. The mixture was shaken in a water bath shaker at 120 rpm at temperatures of 30, 40, 50, 60, and 70°C for 180 minutes. The mixture was then filtered through Whatman 1 µm porous paper. The filtrate was then centrifuged at 3500 rpm for 15 minutes. Finally, the filtrate was analyzed for lead ion concentration using UV-Vis spectrophotometry.

Evaluation of Adsorbent Capacity

The activation of BBA was carried out using the procedures proposed by Khanday et al. (2017) with modifications. The filtrate was diluted with distilled water in ratios of 1:0 (P1), 1:0.5 (P2), 1:1 (P3), and 1:2 (P4). To achieve a pH of 4.6, 0.1 mol/L acetic acid was added. Approximately 100 mL of diluted filtrate was transferred to each 250 mL Erlenmeyer flask. BBA adsorbent was added in quantities of 9.20 g, 6.57 g, 4.19 g, and 2.01 g for treatments P1, P2, P3, and P4, respectively. Lead ions were absorbed in a water bath shaker at 50°C for 180 minutes at 120 rpm. After adsorption, the mixture was filtered through Whatman 1 µm porous paper and centrifuged at 3500 rpm for 15 minutes. The filtrate was analyzed for lead ion concentration using UV-Vis spectrophotometry

Separation of Solids in Crude Palm Oil Using POME Filtrate

Approximately 42 mL of the adsorbed POME filtrate was incorporated into 158 mL of CPO. The combination of filtrate and CPO was heated and stirred gradually to a temperature of 90-95°C. The mixture was subsequently centrifuged at 3500 rpm for 15 minutes, and the oil layer was isolated. The filtrate was examined for free fatty acids, moisture content, impurities, DOBI (Deterioration Bleachability of Index), and lead levels.

Scanning Electron Microscope Analysis of Boiler Bottom Ash

BBA was placed on carbon tape at the top of the specimen holder for drying, followed by coating with Au. The sample was then transferred to an auto coater until the vacuum coater reached a pressure of 3.2 Pa. The coating process was carried out for 120 seconds, and electrons were fired at BBA with a certain-level probe, followed by evaluation of surface topography.

Energy Dispersive X-Ray (EDX) KOH-Activated Boiler Botton Ash

All samples were sputter-coated with a carbon layer using an Auto Coater JEOL JEC-3000FC to improve electrode conductivity and improve final picture clarity. Sample analysis was conducted with SEM JEOL JSM-6510LA at an accelerating voltage of 5 kV (Bota et al., 2020).

Lead Metal Ion Analysis

A combination of 30 mL of filtrate and 1.5 mL of HNO3 was subjected to destruction until the solution attained a distinct yellow hue. The destroyed filtrate was processed using Whatman 1 µm porous paper. Subsequently, distilled water was added to the filter until its volume reached 30 mL. A total of 2 mL of filtrate were collected, 70 mL of distilled water were included, and 0.1 mol/L NaOH solution was incrementally added until pH reached 4, 6, 7, and 8. Approximately 1 mL of 0.1 mol/L Alizarin Red S solution was introduced, and lead metal ions were examined utilizing UV-Vis Spectrophotometer at wavelengths of 422 nm (pH 4.6), 517 nm (pH 7), and 518 nm (pH 8). The control solution

for each treatment was processed using an identical manner, without the addition of filtrate.

Analysis of Lead in Crude Palm Oil

A total of 2 g of CPO was measured in a 125 mL Erlenmeyer flask. Approximately 10 mL of HNO3, 3 mL of H2O2, and 1 mL of H2SO4 were introduced into the Erlenmeyer flask containing the sample. The mixture was cooked on a hotplate at 150°C for 1.5 hours with a stirring speed of 80 rpm (Yusairi, 2022). The degraded CPO was subjected to cooling and filtration utilizing the Whatman 42 paper. Approximately 2 mL of filtrate was combined with 70 mL of distilled water. Subsequently, a 0.1 mol/L NaOH solution was administered dropwise till achieving a pH of 4.6, followed by the addition of 1 mL of 0.1 mol/L Alizarin red S. The concentration of lead was quantified using UV-Vis spectrophotometer at a wavelength of 422 nm.

Free Fatty Acid Analysis (SNI 01-2891-1992)

A total of 7 g ± 0.02 CPO was weighed in 125 mL Erlenmeyer, followed by the addition of 50 mL of neutral alcohol and 2 drops of phenolphthalein indicator. CPO was then subjected to a temperature of 40°C and titrated with 0.1 N NaOH solution until a persistent pink hue was observed for 30 seconds. The content of free fatty acids (FFA) was determined using the subsequent Equation 1.

$$\% \text{ FFA} = \frac{\text{mL NaOH x N x 256}}{\text{Sample weight x 1000}} \text{ x 100} \quad (1)$$

where mL NaOH was the amount of NaOH solution used, and N was the normality of NaOH.

Analysis of Impurity Content (Gravimetric Method)

The crucible, covered with Whatman 1 µm porous paper, was dried in an oven at 105°C for 60 minutes. It was then cooled in a desiccator for 15 minutes. The mass of the crucible and porous paper (B) was recorded. A 10 g sample of crude palm oil (CPO) (C) was weighed into a glass beaker, and 50 mL of isohexane was added until complete dissolution occurred. The dissolved CPO was then filtered through the crucible lined with porous paper. After filtration, the crucible and porous paper were dried in an oven at 105°C for 30 minutes, followed by cooling in a desiccator for 15 minutes. The final mass of the dry crucible and porous paper (A) was recorded, and the impurity content was calculated using Equation 2.

$$\% \text{ Impurity} = \frac{\text{A}-\text{B}}{\text{C}} \times 100\% \quad (2)$$

where A was the weight of dry porous paper, crucible, and sample, B was the weight of dry and crucible porous paper, and C was CPO weight.

Moisture Content Analysis

The 50 mL glass beaker was subjected to heating in an oven for 3 hours at 105°C. The glass beaker was subjected to cooling in a desiccator for 15 minutes. The cooled beaker (W1) was weighed, and a total of 10 g of CPO (W2) were measured in the glass beaker. CPO and the glass beaker were subjected to heating in the oven for 3 hours at 105°C and were subjected to cooling in a desiccator for 15 minutes, after weighing (W3). The water content was determined using the subsequent Equation 3.

$$\text{Moisture content } (\%) = \frac{(\text{W1}+\text{W2})-\text{W3}}{\text{W2}} \times 100\% \quad (3)$$

where w_1 = beaker weight, w_2 = CPO weight, and w_3 = weight of sample and beaker.

DOBI Analysis (Spectrophotometer Method)

CPO Crude palm oil (CPO) was heated on a hotplate to 55°C and transferred into a 25 mL volumetric flask, with a measured mass of 10 g. Iso-octane was then added to the flask up to the calibration mark. The solution was shaken until the CPO was fully dissolved and subsequently transferred into a cuvette, filling approximately three-quarters of its upper limit. The absorbance was measured using a UV-Vis spectrophotometer at wavelengths of 269 nm and 446 nm, with a sample containing iso-octane serving as the blank. The DOBI value was then calculated using Equation 4.

$$\text{DOBI} = \frac{\text{Absorbance at 446 nm}}{\text{Absorbance at 269 nm}} \quad (4)$$

RESULTS AND DISCUSSION

Scanning Electron Microscope KOH-Activated Boiler Bottom Ash

Figure 1a is SEM of the control BBA, while Figure 1b is BBA activated with 0.4 mol/L KOH. SEM results shows that the control BBA had a smaller pore shape with a rough surface. Other components still cover the pores on the surface of BBA because organic matter decomposes during the combustion process of palm kernel shells and fibers in boiler furnace. Some of the results of the decomposition of organic matter are still

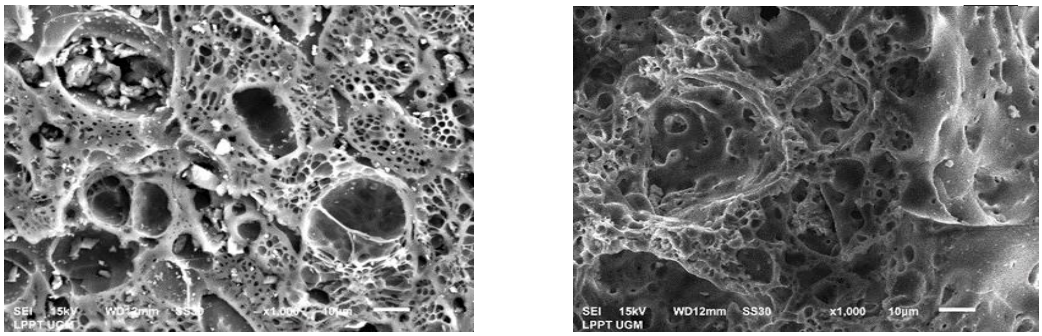

(a) (b)

Figure 1. SEM analysis of control (a) and 0.4 mol/LKOH-activated BBA (b)

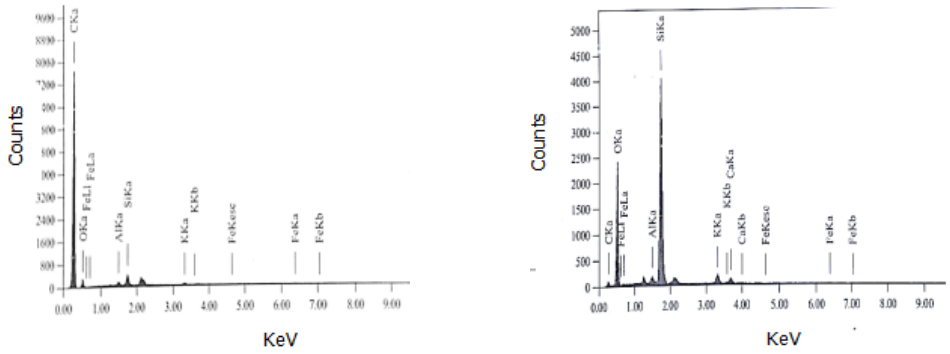

(a) (b)

Figure 2. EDX analysis of control (a) and activated 0.4 mol/LKOH BBA (b)

left behind and stuck to the pore surface of BBA. Some of the results of the decomposition of organic matter become volatile components and are released into the air to form new pores (Marsh, 2006). The activation of BBA is often carried out to remove components that are still left in the pores. Activation of BBA with 0.4 mol/L KOH leads to a cleaner surface with slightly enlarged pores (Figure 1b). The physical changes in the surface of activated BBA are due to the components on the surface and inside BBA pore having been degraded by KOH and then released with KOH leaving the pore (Chiang and Juang, 2017).

Energy Dispersive X-Ray (EDX) KOH-Activated Boiler Botton Ash

The results of EDX analysis of control and 0.4 mol/L KOH-activated BBA are shown in Figures 2(a) and 2(b). The control BBA has a higher carbon element peak than the activated BBA, and the carbonization process increases the carbon element. However, the activation of BBA with KOH leads to a decrease in carbon, and this can be seen from the lower carbon peak of activated BBA compared to BBA. Following the reduction in carbon content, an increase in silicon (Si) and oxygen (O) is observed in activated BBA. These results confirm the weak aggregation of Si onto BBA surface induced by KOH. Si aggregation is due to the destruction of the glassy layer on the surface of BBA, forming active groups inside the pore, such as silica and alumina, coming out to the surface of BBA (Goñi et al., 2003).

Effect of KOH on Activation of Boiler Botton Ash on Lead Adsorption

Figure 3 shows that the adsorbent's ability to bind lead increases by 1.7 times, 1.9 times, and 1.3 times for pH 4, 6, 7, and 8, respectively, with an increase in KOH concentration from 0 to 0.4 M. This is due to the activation of BBA with KOH up to 0.4 M, which removes organic matter that closed the pores of the particles (Figure 1b). However, the increase in KOH concentration from 0.4 to 0.8 mol/L decreases the adsorption of activated BBA by 12.6 times, 8 times, and 5.7 times for pH 4, 6, 7, and 8. This is due to the high KOH concentration damaging the surface of BBA particles and forming a mesoporous structure on the particles. The increase in mesoporous structure leads to

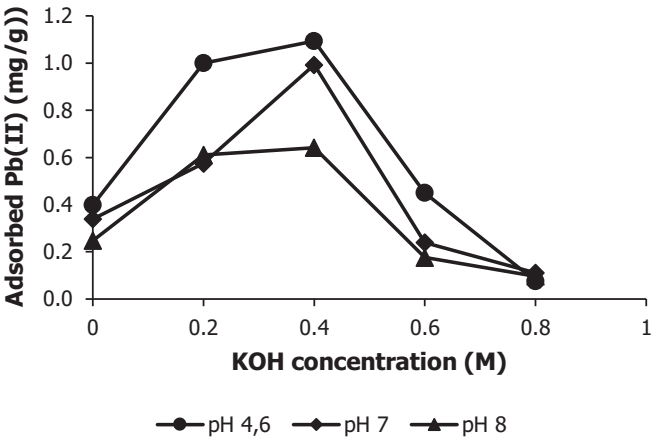

Figure 3. Impact of KOH concentration and solution pH on lead adsorption

reduced particle surface area and decreased adsorption capacity. The best KOH concentration is obtained at 0.4 mol/L for all pH treatments. The best adsorption capacity is obtained at pH 4.6, namely 1.093 mg/g, and the decrease in adsorption capacity at high KOH concentrations is similar to Santoso et al. (2014).

The pH significantly influences the adsorption of lead, as shown in Figure 3. As the pH increases from 4.6 to 8, lead adsorption onto activated BBA decreases, with optimal adsorption occurring at pH 4.6. This effect is attributed to pH-dependent changes in the surface charge of the adsorbent, the ionic charge of lead, and the degree of ionization of solution components (Enache et al., 2017). Under acidic conditions, lead ions remain ionized and positively charged, enhancing their interaction with the adsorbent surface. However, in alkaline conditions, an increased presence of hydroxide ions (OH^-) facilitates the formation of $Pb(OH)^+$, $Pb(OH)_2$, and $Pb(OH)_3^-$ complexes (Fu et al., 2016). This interaction leads to the precipitation of lead hydroxides, thereby inhibiting further adsorption onto the adsorbent surface. Several previous studies have confirmed that the highest adsorption of lead ions occurs at an acidic pH range of 4–5 (Jiménez et al., 2019, Mwamulima et al.,2018, Tasar and Ozer, 2020).

IMPACT OF ADSORBENT AMOUNT ON LEAD ADSORPTION

Figure 4 shows the impact of the adsorbent quantity on the adsorption of lead. Augmenting the adsorbent quantity from 0.5 g to 2 g leads to a 1.77-fold increase in the adsorption of lead. An additional increase in the quantity of adsorbent does not considerably enhance the adsorption of lead. This occurs because adsorbent particles can collect or accumulate owing to an excessive quantity of adsorbent. The aggregation of particles and accumulation of adsorbent materials leads to a reduction of the adsorbent's surface area and concealment of active functional groups, hindering the interaction of lead with these groups on the adsorbent surface. A comparable finding has been documented by Araga et al. (2017).

Adsorbent Capacity

According to Figure 5, the impact of lead concentration in solution at equilibrium leads to adsorption at various adsorption temperatures. Increasing the concentration of lead significantly increases the adsorption of lead metal ions until equilibrium conditions are reached. This is because the amount of lead in the solution exceeds the available adsorbent capacity. The adsorbent can reach saturation point, and the absorption efficiency decreases (Lestari et al., 2020).

The maximum capacity of the adsorbent towards lead is relatively the same at 30°C, 40°C, and 50°C, namely 0.43 mg/g. However, a further increase in adsorption temperature (60°C and 70°C) causes the adsorption of lead to decrease to 0.35 mg/g, which indicates that adsorption is exothermic (Taşar and Özer, 2020, Araga et al., 2017).

The increase in temperature affects the adsorption speed of lead (Figure 5). This can be seen from the adsorption velocity constant value increasing from 3.07 to 5.97 per minute with an increase in adsorption temperature from 30°C to 50°C. However, increasing the adsorption temperature from 50°C to 70°C leads to a constant drop in adsorption velocity to 1.2 per minute. This is because the increase in adsorption temperature elevates the kinetic energy of molecules in the solution,

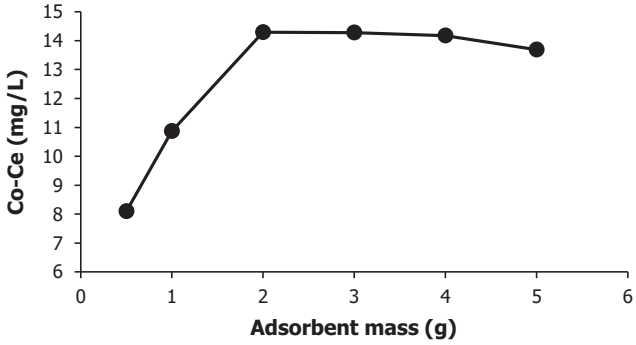

Figure 4. Adsorbed lead metal (Co-Ce) as a function of adsorbent mass. Co represented the starting concentration, while Ce was the concentration at equilibrium.

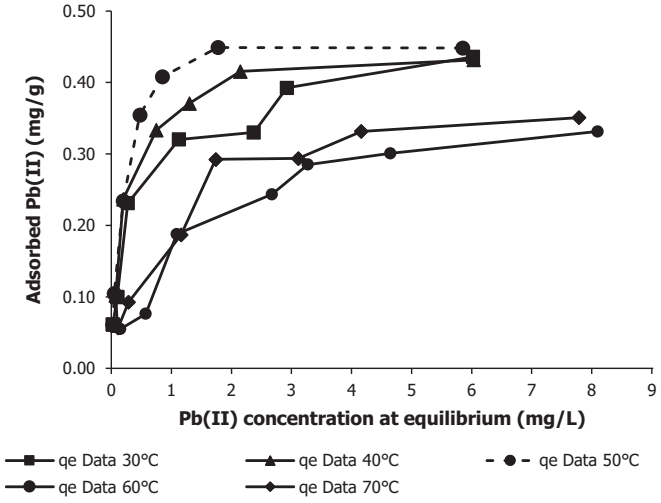

Figure 5. Impact of lead concentration at equilibrium on lead adsorption capacity at various adsorption temperatures

specifically lead, and the movement of adsorbate molecules is faster. Increased molecular movement can increase the intensity of collisions between adsorbate and active groups on the adsorbent surface, leading to higher adsorption (Taşar and Özer, 2020). However, at higher temperatures, the increase in kinetic energy of the particles in the solution causes the particles to move faster. Consequently, the adsorbates are successfully adsorbed by the adsorbent to be released back from the surface of the adsorbent pores (Aisyahlika et al., 2020).

Lead Adsorption Isotherm

Adsorption isotherm of activated BBA on lead is performed at temperatures ranging from 30 °C to 70 °C (Figure 5). The adsorption data indicates adherence to the Langmuir model. Based on the Langmuir isotherm adsorption model, the adsorption rate constants are 3.07, 5.54, 5.97, 1.20, and 1.20 per minute at 30, 40, 50, 60, and 70 °C, respectively. Furthermore, the Arrhenius equation is used to determine the impact of temperature on the adsorption rate constant. The regression of the Arrhenius equation shows that the adsorption activation energy (Ea) is -28675.82 J/mol, while the value of the Arrhenius constant (kA) is 0.0001.

The Ea and kA values are used to predict the adsorption of lead at various temperatures. Figure 6 shows that the Langmuir adsorption isotherm model is suitable for lead adsorption at 60 and 70 °C. However, the obtained Langmuir model is unsuitable for 30, 40, and 50 °C temperatures. This can be because lead adsorption on activated BBA adsorbent is exothermic (Taşar and Özer, 2020, Araga et al., 2017). Based on the adsorption at the best condition, every 1 g of bottom ash adsorbent can reduce the binding of lead metal ions by 0.333 mg lead.

Use of POME Filtrate on Quality of Crude Palm Oil

POME contains higher lead than standard water, and adsorption of lead on POME using activated BBA adsorbent reduces lead in the filtrate. The use of POME filtrate purified using BBA adsorbent as water dilution for CPO quality is presented in Table 1. Filtrate without dilution, as used for water dilution, gives significant differences in lead content. The moisture content, impurity content, DOBI, and lead of CPO after treatment are in the specified quality standards in all treatments. FFA content in all treatments is higher than the specified quality standard, which is a maximum of 5%.

The high FFA value in CPO is due to decreasing the quality of the raw material during storage and oil separation. High moisture content can increase the activity of lipases that hydrolyze triglycerides into FFAs. In addition, high moisture also creates an ideal environment for the growth of microorganisms that accelerate fat hydrolysis. High contaminant matter levels can also act as a catalyst for triglyceride hydrolysis reactions. These factors accelerate the formation of FFA (Juniarto and Isnasia, 2021).

Using POME filtrate without dilution for water dilution in separating oil and sludge significantly affects lead content in CPO. This is because POME filtrate without dilution still has lead concentration higher than the specified quality standard (1 mg/L) and lead in POME filtrate is diffused into CPO during the sludge separation

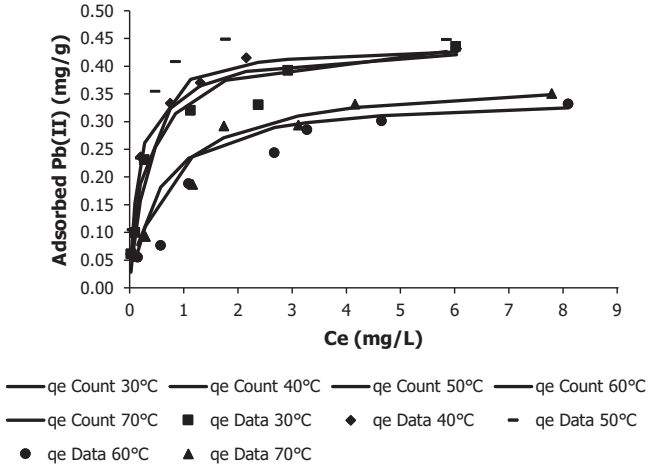

Figure 6. Langmuir model of lead adsorption on BBA adsorbent as a function of lead solution concentration. Therefore, qe count was a calculated adsorbed lead, and qe data was experimental data.

Table 1. Impact of POME as water dilution on CPO quality

Ratio CPO: POME*	Free fatty acid	Moisture content	Impurity content	DOBI	Lead
1:0	5.24 ± 0.03[a]	0.24 ± 0.01[a]	0.17 ± 0.02[a]	2.27 ± 0.01[a]	0.33 ± 0.04[b]
1:0.5	5.22 ± 0.02[a]	0.23 ± 0.05[a]	0.16 ± 0.01[a]	2.31 ± 0.02[a]	0.23 ± 0.09[a]
1:1	5.24 ± 0.02[a]	0.23 ± 0.07[a]	0.16 ± 0.01[a]	2.29 ± 0.03[a]	0.22 ± 0.02[a]
1:2	5.24 ± 0.01[a]	0.22 ± 0.02[a]	0.16 ± 0.02[a]	2.30 ± 0.01[a]	0.22 ± 0.05[a]
Water	5.23 ± 0.02[a]	0.21 ± 0.01[a]	0.15 ± 0.02[a]	2.30 ± 0.01[a]	0.21 ± 0.03[a]
Standard**	Maximum 5.0%	Maximum 0.25 %	Maximum 0.25 %	Minimum 2.2	Maximum 0.1 mg/kg

*POME was purified with BBA adsorbent. **The standard was SNI-01-2901-2006 except for Lead (SNI 7709: 2012). Notes: The data was presented as means ± standard deviation (n = 15). Distinct letters in the same row signify substantial differences determined using one-way ANOVA with Tukey's HSD post hoc test ($p<0.05$). Distinct letters in the same row signified substantial differences ($P<0.05$). DOBI (Deterioration Bleachability of Index).

process. Separating oil and sludge using distilled water and diluted POME filtrate as water dilution does not substantially influence lead content of CPO produced. Lead in vegetable oil is generally due to contamination from natural sources and plantation activities (fertilization and herbicide spraying) during harvesting, transport, and processing. (Yang et al., 2016).

CONCLUSION

In conclusion, SEM analysis of activated BBA using 0.4 mol/LKOH led to a cleaner particle surface with slightly larger pores than the control. Evaluation using EDX showed a weak degree of aggregation of Si onto the surface of activated BBA and a decrease in carbon followed by an increase in Si and O. In addition, the best KOH concentration was obtained at 0.4 mol/L for all pH treatments, with the most adsorption occurring at pH 4.6. The adsorbent's maximal capacity remained consistent at 30°C, 40°C, and 50°C, which was about 0.43 mg/g. However, a further increase in adsorption temperature (60°C and 70°C) caused the adsorption of lead to decrease to 0.35 mg/g which showed that adsorption was exothermic. In addition, the temperature rise influenced the adsorption rate of lead which rose from 3.07 to 5.97 per minute when the adsorption temperature elevated from 30°C to 50°C. Elevating the temperature from 50°C to 70°C reduced the adsorption velocity constant to 1.2 per minute, and the adsorption of lead adhered to the Langmuir isotherm model. The adsorption rate constants were 3.07, 5.54, 5.97, 1.20, and 1.20 per minute for temperatures of 30, 40, 50, 60, and 70°C, respectively. The adsorption activation energy (Ea) value was -28675.82 J/mol, and the Arrhenius constant (kA) value was 0.0001. The use of POME filtrate with and without the addition of water as water dilution did not affect FFA, moisture content, contaminant content, and DOBI. However, the treatment without dilution made a difference in lead content. The results indicated that BBA activated with KOH could serve as an adsorbent to diminish lead concentration in POME. POME purified with BBA adsorbent could be used as diluent water in CPO processing process to reduce raw water use, ultimately reducing POME production.

CONFLICT OF INTEREST

The authors asserted no conflict of interest for the submitted work entitled " Boiler Ash of Oil Palm Shell as Adsorbent for Lead Adsorption ".

REFERENCES

Aisyahlika, S. Z., Firdaus, M. L., & Elvia. R. (2018). Kapasitas Adsorpsi Arang Aktif Cangkang Bintaro (Cerbera odollam) Terhadap Zat Warna Sintetis Reactive Red-120 dan Reactive Blue-198. *Pendidikan Dan Ilmu Kimia*, *2*(2): 148–155. https://ejournal.unib.ac.id/alotropjurnal/article/view/7483/3700

Araga, Ramya., Shantana Soni & Chandra S. Sharma. (2017). Fluoride Adsorption from Aqueous Solution using Activated Carbon Obtained from KOH-treated Jamun (Syzygium cumini) Seed. Journal of Environmental Chemical Engineering, *5*(6): 5608-5616. https://www.sciencedirect.com/science/article/pii/S2213343717305249?via%3Dihub

Asyri, F., Hafni, K. N., & Simamora, A. H. (2015). Pengaruh Limbah Abu Pembakaran Biomassa Kelapa Sawit Terhadap Sifat-Sifat Fisika dan Mekanik High Impact

Polystyrene. *Jurnal Teknik Kimia USU*, *4*(3): 23-28. https://talenta.usu.ac.id/jtk/article/view/1477/957

Botha, E., Smith, N., Hlabano-Moyo, B., & Bladergroen, B. (2020). The impact of Slurry Wet Mixing Time, Thermal Treatment, and Method of Electrode Preparation on Membrane Capacitive Deionisation Performance. Processes 2021, 9, 1. https://dx.doi.org/10.3390/pr9010001

Chen, G., & Shi, L. (2017). Removal of Cd(II) and Pb^{2+} ions from natural water using a low-cost synthetic mineral: Behavior and mechanisms. *RSC Advances*, *7*(69): 43445–43454. https://doi.org/10.1039/c7ra08018b

Chiang, Y. C., & Juang, R. S. (2017). Surface modifications of carbonaceous materials for carbon dioxide adsorption: A review. *Journal of the Taiwan Institute of Chemical Engineers*, *71*: 214–234. https://doi.org/10.1016/j.jtice.2016.12.014

Durán-Jiménez, G., Hernández-Montoya, V., Rodríguez Oyarzun, J., Montes-Morán, M. Á., & Binner, E. (2019). Pb^{2+} removal using carbon adsorbents prepared by hybrid heating system: Understanding the microwave heating by dielectric characterization and numerical simulation. *Journal of Molecular Liquids*, *277*: 663–671. https://doi.org/10.1016/j.molliq.2018.12.143

Elysabeth, T., Jufrodi., & Hudaeni. (2015). Adsorbsi Logam Berat Besi dan Timbal Menggunakan Zeolit Alam Bayah Teraktivasi. *Jurnal Chemtech*, *1*(1) 26-29. https://e-jurnal.lppmunsera.org/index.php/Chemtech/article/view/7/5

Enachea, D.F., Vasilea, E., Simonescua, C.M., Răzvana, A., Nicolescub, A., Nechifora, A.C., Opreaa, O., Pătescua, R.E., Onosea, C., & Dumitru, F. 2017. Cysteine-functionalized silica-coated magnetite nanoparticles as potential nano-adsorbents. *Journal of Solid State Chemistry*. Volume 253. Pages 318-328. https://www.sciencedirect.com/science/article/pii/S0022459617302359?via%3Dihub

Firmana, F., Rizhanb, M., & Sahidia, A.A. (2020). Analisis Kandungan Logam Berat Abu Batubara Pltu Bangko Barat Kab. Muara Enim Sumatera Selatan. *Journal of Science and Engineering*, *3*(1): 10–16. https://ejournal.unkhair.ac.id/index.php/josae/article/view/2070/1507

Fu, R., Liu, Y., Lou, Z., Wang, Z., Baig, S. A., & Xu, X. (2016). Adsorptive removal of Pb^{2+} by magnetic activated carbon incorporated with amino groups from aqueous solutions. *Journal of the Taiwan Institute of Chemical Engineers*, *62*: 247–258. https://doi.org/10.1016/j.jtice.2016.02.012

Gautam, R. K., Mudhoo, A., Lofrano, G., & Chattopadhyaya, M. C. (2014). Biomass-derived biosorbents for metal ions sequestration: Adsorbent modification and activation methods and adsorbent regeneration. In *Journal of Environmental Chemical Engineering*, *2*(1): 239–259. Elsevier Ltd. https://doi.org/10.1016/j.jece.2013.12.019

Goñi, S., Guerrero, A., Luxán, M. P., & Macías, A. (2003). Activation of the fly ash pozzolanic reaction by hydrothermal conditions. *Cement and Concrete Research*, *33*(9): 1399–1405. https://doi.org/10.1016/S0008-8846(03)00085-1

Juniarto, T., & Isnasia, I. D. (2021). Uji Kualitas Minyak Goreng Sawit Yang Beredar di Entikong Kalimantan Barat. *Food Scientia : Journal of Food Science and Technology*, *1*(2): 117–130. https://doi.org/10.33830/fsj.v1i2.1916.2021

Khanday, W. A., Marrakchi, F., Asif, M., & Hameed, B. H. (2017). Mesoporous zeolite–activated carbon composite from oil palm ash as an effective adsorbent for methylene blue. *Journal of the Taiwan Institute of Chemical Engineers*, *70*: 32–41. https://doi.org/10.1016/j.jtice.2016.10.029

Lestari, I., Mahraja, M., Farid, F., Gusti, D. R., & Permana, E. (2020). Penyerapan Ion Pb (II) Menggunakan Adsorben Dari Limbah Padat Lumpur Aktif Pengolahan Air Minum. *Chemistry Progress*, *13*(2). https://doi.org/10.35799/cp.13.2.2020.31391

Mahmud, E., Huq, A.K.O., & Rosiyah. 2016. The removal of heavy metal ions from wastewater/ aqueous solution using polypyrrole-based adsorbents. *Journal RSC Advances*. Issue 18. 14778–14791.

Marsh H, R.-R.F. 2006. Activated carbon. Elsevier Science & Technology Books, Great Britain

Mwamulima, T., Zhang, X., Wang, Y., Song, S., & Peng, C. (2018). Novel approach to control adsorbent aggregation: iron fixed bentonite-fly ash for Lead (Pb) and Cadmium (Cd) removal from aqueous media. *Frontiers of Environmental Science and Engineering*: *12*(2). https://doi.org/10.1007/s11783-017-0979-6

Myllymäki, P., Lahti, R., Romar, H., & Lassi, U. (2018). Removal of total organic carbon from peat solution by hybrid method-Electrocoagulation combined with adsorption. *Journal of Water Process Engineering*, 24: 56–62. https://doi.org/10.1016/j.jwpe.2018.05.008

Nursanti, I. 2013. Karakteristik Limbah Cair Pabrik Kelapa Sawit Pada Proses Pengolahan Anaerob dan Aerob. *Jurnal Ilmiah Universitas Batanghari Jambi. 13*(4): 67-73.

Oktasari, A. (2018). Kulit Kacang Tanah (Arachis hypogaea L.) sebagai Adsorben Ion Pb2+. Jurnal Ilmu Kimia dan Terapan, *2*(1): 17-27. https://jurnal.radenfatah.ac.id/index.php/alkimia/article/view/2258/1599

Permata, A.N., Adinda P.P, R.R., & Takwanto, A. 2019. Studi Awal Pengaruh Suhu dan Konsentrasi Pada Proses Aktivasi Karbon Dari Kayu Halaban Menggunakan $ZNCL_2$ dan KOH. Jurnal Teknologi Separasi,.5 (2),141-146.

Praipipat, P., Jangkorn, S., & Ngamsurach, P. (2023). Powdered and beaded zeolite A from recycled coal fly ash with modified iron (III) oxide-hydroxide for Lead

adsorptions. Environmental Nanotechnology, Monitoring & Management, *20*: 100812. https://www.sciencedirect.com/science/article/pii/S2215153223000363

Prianti, E., Malino, M. B., & Lapanporo, B., P. (2015). Pemanfaatan Abu Kerak Boiler Hasil Pembakaran Limbah Kelapa Sawit Sebagai Pengganti Parsial Pasir pada Pembuatan Beton. *Positron*, *V* (1): 26–29. https://jurnal.untan.ac.id/index.php/jpositron/article/view/9744

Ray, P. Z., & Shipley, H. J. (2015). Inorganic nano-adsorbents for the removal of heavy metals and arsenic: A review. *RSC Advances*, *5*(38): 29885–29907. https://doi.org/10.1039/c5ra02714d

Santoso, R.H., Susilo, B., & Nugroho, W.A. (2014). Pembuatan dan Karakterisasi Karbon Aktif dari Kulit Singkong (Manihot esculenta Crantz) Menggunakan Activating Agent KOH. Jurnal Keteknikan Pertanian Tropis dan Biosistem, *2*(3): 279-286. https://jkptb.ub.ac.id/index.php/jkptb/article/view/236/200

Suparma, B. L., Panggaben, T. W., & Mude, S. (2014). Potensi Penggunaan Limbah Kelapa Sawit Sebagai Agregat Pengisi Pada Campuran Hot Rolled Sheet-Base. *Jurnal Transportasi*, *14*(2), 87–96. https://www.researchgate.net/publication/301632904

Taşar, Ş., & Özer, A. (2020). A thermodynamic and kinetic evaluation of the adsorption of Pb2+ions using peanut (Arachis hypogaea) shell-based biochar from aqueous media. *Polish Journal of Environmental Studies*, *29*(1): 293–305. https://doi.org/10.15244/pjoes/103027

Wijaya, I.K., Yulia, Y.F., & Udyani, K. 2020. Pemanfaatan Daun Teh Sebagai Biosorben Logam Berat Dalam Air Limbah (Review). *Jurnal Envirotek. 12(2)*: 25-33.

Yang, Y., Li, H., Peng, L., Chen, Z., & Zeng, Q. (2016). Assessment of Pb and Cd in seed oils and meals and methodology of their extraction. *Food Chemistry*, *197*: 482–488. https://doi.org/10.1016/j.foodchem.2015.10.143